

# Natural Convection of Double-Diffusive Flow of Heat Generating Fluid in a Vertical Channel

Benjamin Boniface<sup>1,\*</sup>, Abiodun O. Ajibade<sup>2</sup>

<sup>1</sup>Department of Mathematics, Aduvie Pre-University, Jahi District Abuja, Nigeria

<sup>2</sup>Department of Mathematics, Ahmadu Bello University, Zaria, Nigeria

**Abstract** Natural convection double diffusive flow heat generating fluid in a vertical channel has been examined. Diffusion-thermo (Dufour) and heat generating effects are also considered. Suitable transformations are employed to convert the partial differential equations representing the concentration, temperature and velocity into a system of ordinary differential equations. Approximate solutions are obtained for velocity, skin-friction, temperature, heat transfer, concentration and mass transfer by the use of a two-term harmonic and non-harmonic perturbation method. The result for the mixture of carbon dioxide ( $Sc = 0.94$ ) in air ( $Pr = 0.71$ ) are presented graphically. It is found that the velocity decreases with increasing slip ( $\lambda$ ) while it increases with increasing thermal diffusion ( $Df$ ). Also the mean skin-friction  $|M|$  and the phase of the rate of heat transfer  $|N|$  increases with increase in the buoyancy parameter as well as Dufour effect while both the temperature and concentration increase near the hot plate and decreases exponentially towards the cold plate.

**Keywords** Natural convection, Double-diffusive, Heat generating and Dufour effect

## 1. Introduction

Double-diffusive convection flows are generated by buoyancy effect caused by combined temperature and concentration gradients. It finds its application in oceanography process, multi-component convection flows induced by density gradient and some technological applications.

In literature, the wide range applications of double-diffusive convection is well reported in [1-5], Boutana et al [6], reported that for multiple solutions, the variety of buoyancy ratios is dependent on the kind of convection generated by the solute gradients. Similarly, Nithyaderi and Yang [7] investigated double-diffusive natural convection in a partial heated enclosure with sores and Dufour effects. Jha et al [8] examined the role of thermal diffusive on double-diffusive natural convection in a vertical annular porous medium.

On the other hand, several investigations have been made on natural convective heat transfer to viscous incompressible slip flow past a channel. This is due to useful applications in electric cooling, heat exchangers and physiological type flows and so on. Jha et al [9] studied free convection flow of

heat generating absorbing fluid between vertical porous plate with periodic heat input. Under sores and dufour effect, Hayat. et al [10] studied Melting heat transfer in a boundary layer flow while Jha and Ajibade [11], studied free convection flow between Heat and Mass Transfer Flow in a vertical Channel with Dufour effect. Similarly, Ajibade [12], examined Dual-phase-lag and dufour effects on unsteady double-diffusive convection flow in a vertical micro-channel filled with porous material, Also, the influence of periodic temperature and concentration on free convection, flow and heat transfer past a vertical plate in slip-flow region was presented by Sharma [13]. Srinivasa and Eswara, [14] studied unsteady free convection flow and heat transfer from an isothermal truncated cone with variable viscosity. Hossain et al [15] surveyed the influence of fluctuating surface temperature and concentration on natural convection flow from a vertical flat plate. Moreover, Sharma and Chaudhary [16] examined the effect of variable suction on transient free convective viscous incompressible flow past a vertical plate with periodic temperature variations in slip-flow regime, While Anwar [17] investigated MHD unsteady free convective flow past a vertical porous plate. Also, Soundalgekar and Wavre [18,19] presented the unsteady free convection and mass transfer flow past an infinite vertical plate with constant and variable suction, while, Chen et al [20] investigated ,the combined heat and mass transfer in mixed convective flow along an inclined plate. More details on velocity slip and temperature jump are found in Haddad et al [21,22]. Similarly, heat generating and heat transfer was studied by the following people. Ogulata

\* Corresponding author:

benboninc@gmail.com (Benjamin Boniface)

Published online at <http://journal.sapub.org/ajms>

Copyright © 2019 The Author(s). Published by Scientific & Academic Publishing

This work is licensed under the Creative Commons Attribution International

License (CC BY). <http://creativecommons.org/licenses/by/4.0/>

and Dabo [23] investigated Experiment and entropy generation minimization analysis of a cross flow heat exchanger. Flow and heat transfer characteristics of transverse perforated rids under impingement was studied by Caliskan [24], while Heat/mass transport in a drop translating in time-periodic electric field was found by Abdelaal and Jog [25]. Zambra and Moraga [26], Examined Heat and mass transfer in landfills simulation of the pile self-heating and of soil contamination. Conjugate heat transfer in a plate –one surface at constant temperature and the other cooled by forced or natural convection was studied by Matti and Reijo [27]. Hadi and Jerzy [28], investigated Maximization of heat transfer across micro-channels. Mohamed and Tassos [29], studied Heat transfer correlation for flow boiling in small to micro tube. Alessandra and Augusta [30], investigated Mass/heat transfer through laminar boundary layer in ax symmetric micro channels with non uniform cross section and fixed wall concentration/temperature. Heat transfer mechanism in pool boiling and solidification is found in Heui-seol [31,32].

In the work Sharma [13], there is velocity slip on the boundary plate. However, due to partial contact between the plate and fluid particles which is caused by the slip, it is expected that there is temperature as well as concentration jumps on the boundary as well. This fact was not addressed in [13], which motivate the authors to conduct the present research.

The objective of the present investigation is to study Natural convection double-diffusive flow of heat generating fluid in a vertical channel, considering the velocity slip, as well as boundary jump in temperature and concentration.

## 2. Formulation of the Problem

Double-diffusive free convective flow of heat generating fluid in a vertical channel is considered.

The  $x^*$  - axis is taken in vertical upward direction along the vertical porous plate and  $y^*$  - axis is taken normal to the plate. The plates are considered infinite in the  $x^*$  - direction so that all physical quantities are dependent on  $y^*$  and  $t^*$  only. In the present problem, the fluid temperature is governed by mass flux, hence the Dufour effect is considered in the energy equation. Neglecting viscous dissipation and then assuming variation of density in the body force term (Boussinesq's approximation) the problem is governed by the following set of equations.

$$\frac{\partial U^*}{\partial t^*} + V^* \frac{\partial U^*}{\partial y^*} = g\beta(T^* - T_\infty^*) + g\beta^0(C^* - C_\infty^*) + \nu \frac{\partial^2 U^*}{\partial y^{*2}} \quad (1)$$

$$\frac{\partial T^*}{\partial t^*} + V^* \frac{\partial T^*}{\partial y^*} = \frac{1}{\rho C_p} \left[ K \frac{\partial^2 T^*}{\partial y^{*2}} + D \frac{\partial^2 C^*}{\partial y^{*2}} \right] + \frac{Q_0(T^* - T_0)}{\rho C_p} \quad (2)$$

$$\frac{\partial C^*}{\partial t^*} + V^* \frac{\partial C^*}{\partial y^*} = Dm \frac{\partial^2 C^*}{\partial y^{*2}} \quad (3)$$

The continuity equation for the present problem is

$$\frac{\partial U^*}{\partial x^*} + \frac{\partial V^*}{\partial y^*} = 0 \quad (4)$$

Since the flow is independent of the  $x^*$  direction,  $\frac{\partial U^*}{\partial x^*}$  vanishes so that continuity equation reduces to

$$\frac{\partial V^*}{\partial y^*} = 0 \quad (5)$$

By integration of (5) we have  $V^*$  to be function of  $t$  only. Following [2], we take

$V^* = -V_0^* (1 + \varepsilon A e^{i\omega t})$ . Where  $V_0$ ,  $\varepsilon$ , and  $A$  are constants.

The boundary conditions for the present problem, considering the velocity slip, boundary jump and steady-periodic heat and concentration input on the boundary are

$$\begin{aligned} U^*(0, t) &= \lambda^* \frac{\partial U^*}{\partial y^*}(0, t) \\ T^*(0, t) &= T_w^* + \varepsilon(T_w^* - T_0^*)e^{i\omega t} + \frac{\lambda^* K}{\rho C_p} \frac{\partial T^*}{\partial y^*}(0, t) \\ C^*(0, t) &= C_w^* + \varepsilon(C_w^* - C_0^*)e^{i\omega t} + \frac{\lambda^* Dm}{K} \frac{\partial C^*}{\partial y^*}(0, t) \end{aligned} \quad (6)$$

$$U^*(y, t) = 0, \quad T^*(y, t) = T_0^*, \quad C^*(y, t) = C_0^* \text{ as } y = H$$

Defining the following dimensionless parameter:

$$\begin{aligned} Gr &= g\beta\nu \frac{(T_w^* - T_0^*)}{V_0^{*3}}, \quad t = \frac{t^* V_0^{*2}}{4\nu}, \quad \lambda = \frac{V_0^* \lambda^*}{\nu} \\ Gc &= g\beta^0\nu \frac{(C_w^* - C_0^*)}{V_0^{*3}}, \quad \theta = \frac{T^* - T_0^*}{T_w^* - T_0^*}, \quad Df = \frac{D}{K} \frac{\Delta C}{\Delta T} \\ Pr &= \frac{\mu C_p}{K} = \frac{\nu \rho C_p}{K}, \quad C = \frac{C^* - C_0^*}{C_w^* - C_0^*}, \quad y = \frac{y^* V_0^*}{\nu} \\ Sc &= \frac{\nu}{Dm}, \quad U = \frac{U^*}{V_0^*}, \quad \omega = \frac{4\nu\omega^*}{V_0^{*2}} \\ \frac{\Delta C}{\Delta T} &= \frac{C_w^* - C_0^*}{T_w^* - T_0^*}, \quad \delta = \frac{Q_0\nu^2}{KV_0^{*2}} \end{aligned} \quad (7)$$

Where (\*) stand for dimensional quantity,  $Gr$  is the Grashof number,  $Gc$  is the modified Grashof number,  $Pr$  is the Prandtl number,  $Sc$  is the Schmidt number,  $\delta$  is heat generating parameter and  $\lambda$  is jump/ slip parameter. All the physical parameters used are defined in the nomenclature.

Upon substitution of equation (7) into the governing equation (1)-(3) and the boundary condition (6), the equations are presented in dimensionless form as

$$\frac{1}{4} \frac{\partial U}{\partial t} - \left(1 + \varepsilon A e^{i\omega t}\right) \frac{\partial U}{\partial y} = Gr\theta + GcC + \frac{\partial^2 U}{\partial y^2} \quad (8)$$

$$\frac{1}{4} \frac{\partial \theta}{\partial t} - \left(1 + \varepsilon A e^{i\omega t}\right) \frac{\partial \theta}{\partial y} = \frac{1}{Pr} \frac{\partial^2 \theta}{\partial y^2} + \frac{Df}{Pr} \frac{\partial^2 C}{\partial y^2} + \frac{\delta}{Pr} \theta \quad (9)$$

$$\frac{1}{4} \frac{\partial C}{\partial t} - \left(1 + \varepsilon A e^{i\omega t}\right) \frac{\partial C}{\partial y} = \frac{1}{Sc} \frac{\partial^2 C}{\partial y^2} \quad (10)$$

While the boundary conditions are reduced to the following dimensionless form:

$$U = \lambda \frac{\partial U}{\partial y}, \quad \theta = 1 + \varepsilon e^{i\omega t} + \frac{\lambda}{Pr} \frac{\partial \theta}{\partial y}, \quad C = 1 + \varepsilon e^{i\omega t} + \frac{\lambda}{Sc} \frac{\partial C}{\partial y},$$

$$\text{at } y = 0 \quad (11)$$

$$U = 0 \quad \theta = 0 \quad C = 0 \quad \text{as } y = H$$

### 3. Solution of the Problem

Assuming small amplitude oscillations ( $\varepsilon \ll 1$ ), we can represent the velocity  $U$ , temperature  $\theta$ , and concentration near the plate.

To obtain the solutions for the velocity, concentration and energy equations (8)-(10), we separate the variables into the harmonic and non-harmonic parts as follows

$$U(y, t) = U_0(y) + \varepsilon U_1(y) e^{i\omega t},$$

$$\theta(y, t) = \theta_0(y) + \varepsilon \theta_1(y) e^{i\omega t} \quad (12)$$

$$C(y, t) = C_0(y) + \varepsilon C_1(y) e^{i\omega t}$$

Now, substituting (12) into (8) to (10), equating the coefficients of harmonic and non-harmonic term, neglecting the coefficient of  $\varepsilon^2$ , we have the following set of ordinary differential equations

$$\theta_0'' + Pr \theta_0' + \theta_0 \delta = -Df C_0''$$

$$\theta_1'' + Pr \theta_1' - \frac{(i\omega Pr - 4\delta)}{4} \theta_1 = -Df C_1'' - A Pr \theta_0'$$

$$U_0'' + U_0' = -Gr \theta_0 - Gc C_0 \quad (13)$$

$$U_1'' + U_1' - \frac{i\omega}{4} U_1 = -Gr \theta_1 - Gc C_1 - A U_0'$$

$$C_0'' + Sc C_0' = 0$$

$$C_1'' + Sc C_1' = \frac{i\omega Sc}{4} C_1 = -A Sc C_0'$$

With the corresponding boundary conditions

$$U_0 = \lambda \frac{\partial U_0}{\partial y}, \quad U_1 = \lambda \frac{\partial U_1}{\partial y}$$

$$\theta_0 = 1 + \frac{\lambda}{Pr} \theta_0', \quad \theta_1 = \frac{\lambda}{Pr} \theta_1' \quad \text{at } y = 0 \quad (14)$$

$$C_0 = 1 + \frac{Kn}{Sc} C_0', \quad C_1 = \frac{\lambda}{Sc} C_1'$$

$$U_0 = 0, \quad U_1 = 0, \quad \theta_0 = 0,$$

$$\theta_1 = 0, \quad C_0 = 0, \quad C_1 = 0, \quad \text{as } y = H$$

Now, solving the ODE (13) using the boundary conditions (14), we get the following results:

$$C_0(y) = B_1 e^{-Scy} + B_2 \quad (15)$$

$$C_1(y) = B_{13} e^{m_3 y} + B_{12} e^{-m_4 y} + B_{11} e^{-Scy} \quad (16)$$

$$\theta_0(y) = B_5 e^{-m_1 y} + B_4 e^{-m_2 y} - B_3 e^{-Scy} \quad (17)$$

$$U_0(y) = B_{10} + B_9 e^{-y} + B_8 e^{-scy} + B_7 e^{-m_2 y} + B_6 e^{m_1 y} - Gc B_2 y \quad (18)$$

$$\theta_1(y) = B_{17} e^{-m_4 y} + B_{14} e^{-m_1 y} + B_{18} e^{-Scy} + B_{15} e^{-m_2 y} + B_{16} e^{m_3 y} + B_{19} e^{-m_6 y} + B_{20} e^{m_5 y} \quad (19)$$

$$U_1(y) = B_{21} e^{m_1 y} + B_{22} e^{-m_2 y} + B_{23} e^{m_3 y} + B_{24} e^{-m_4 y} + B_{25} e^{m_5 y} + B_{26} e^{-m_6 y} + B_{27} e^{-scy} + B_{28} e^{-y} + B_{29} y + B_{30} e^{-m_8 y} + B_{31} e^{m_7 y} \quad (20)$$

So that expressions for the concentration, temperature and velocity are

$$C = B_1 e^{-scy} + B_2 + \varepsilon (B_{13} e^{m_3 y} + B_{12} e^{-m_4 y} + B_{11} e^{-Scy}) e^{i\omega t} \quad (21)$$

$$\theta = B_5 e^{m_1 y} + B_4 e^{-m_2 y} + \varepsilon (B_{17} e^{-m_4 y} + B_{14} e^{m_1 y} + B_{18} e^{-Scy} + B_{16} e^{m_3 y} + B_{19} e^{-m_6 y} + B_{20} e^{m_5 y} + B_{15} e^{-m_2 y}) e^{i\omega t} \quad (22)$$

$$U = B_{10} + B_9 e^{-y} + B_8 e^{-scy} + B_7 e^{-m_2 y} + B_6 e^{m_1 y} - Gc B_2 y + \varepsilon (B_{21} e^{m_1 y} + B_{23} e^{m_3 y} + B_{24} e^{-m_4 y} + B_{25} e^{m_5 y} + B_{26} e^{-m_6 y} + B_{27} e^{-Scy} + B_{22} e^{-m_2 y} + B_{28} e^{-y} + B_{29} y + B_{30} e^{-m_8 y} + B_{31} e^{m_7 y}) e^{i\omega t} \quad (23)$$

All the constants used to define equations (15)-(20) are given in the appendix.

Two main features that are worthy of investigation in this problem are the skin-friction and the rate of heat transfer at the surface of the bounding plates.

**Skin – Friction:** Now, the dimensionless sharing on the surface of a body due to a fluid motion is known as skin-friction and this is defined by the Newton's Law of viscosity.

$$\tau^* = \nu \frac{\partial U^*}{\partial y^*} \quad (24)$$

Now, using equation (23), and then calculating the sharing stress component in dimensionless form as:

$$\tau = \frac{\tau}{\rho V_0^{*2}} = \frac{\partial U}{\partial y} \bigg|_{y=0} \quad (25)$$

Now, considering the amplitude and phase, the skin-friction can be written as

$$\tau = \tau_m + \varepsilon |M| \cos(\omega t + \varphi) \quad \text{Where the Amplitude is } |M| = |M_r + iM_i| \text{ and the Phase of the Skin-friction is } \tan \varphi = \frac{iM_i}{M_r}$$

$$M = M_r + iM_i = B_{21}m_1 - B_{22}m_2 + B_{23}m_3 - B_{24}m_4 + B_{25}m_5 - B_{26}m_6 - B_{27}Sc - B_{28} + B_{29} - B_{30} + B_{31}m_7$$

and the mean skin-friction  $\tau_m$  is denoted

$$\tau_m = B_9 - B_8Sc - B_7m_2 + B_6m_1 + B_2Gc$$

**Heat Transfer:** Knowing that in dynamics of viscous fluid the interest is not much in knowing all the details of the velocity and temperature fields but would therefore like to know quantity of heat exchange between the body and the fluid. Now, at the boundary, the heat exchanged between the fluid and the body is only due to conduction, accordingly, using the Fourier's law, the heat transfers in governed by the equation.

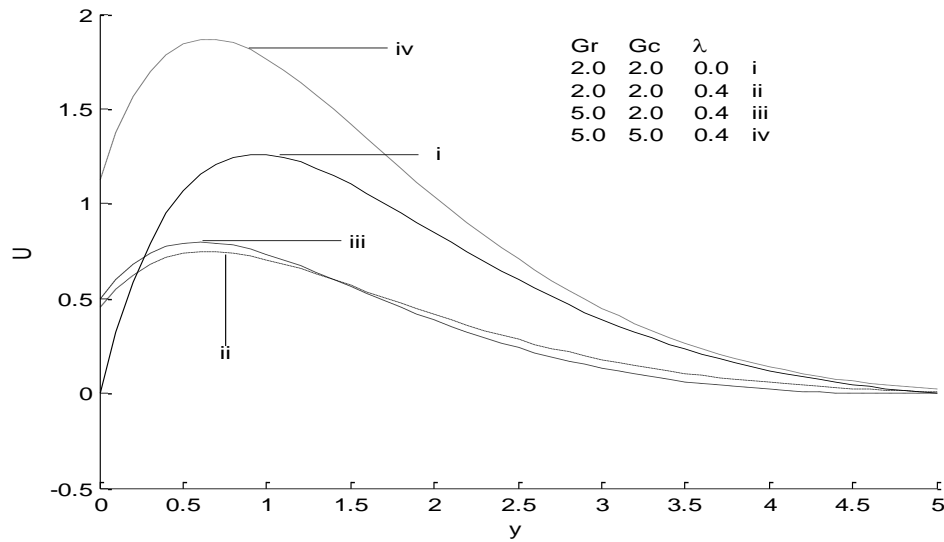


Figure 1. Velocity profiles of carbon dioxide ( $Sc=0.94$ ) in air ( $Pr=0.71$ ), for different values of  $Gr, Gc$  and  $\lambda$ ,  $\omega=10$ ,  $\omega t=0.2$ ,  $A=5$ , and  $\varepsilon=0.02$

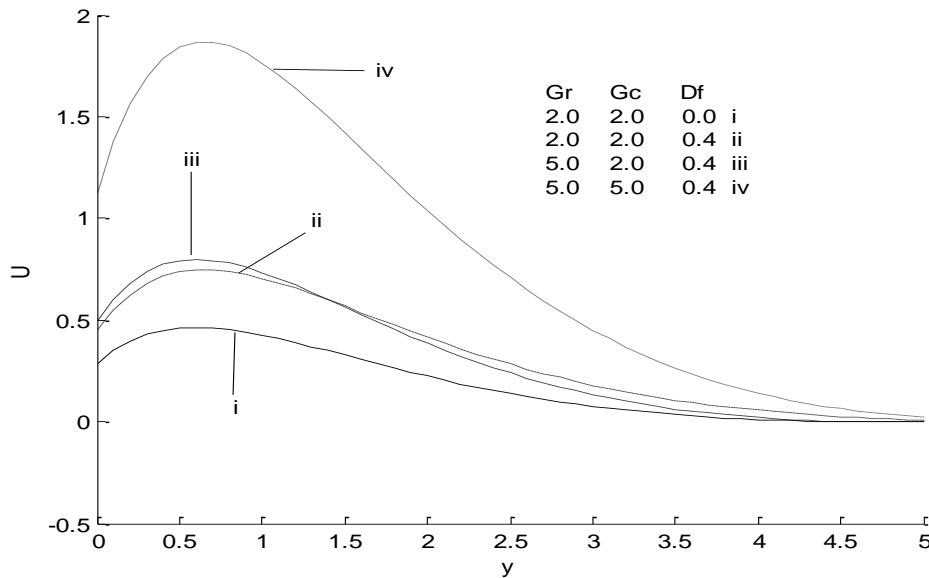


Figure 2. Velocity profiles of carbon dioxide ( $Sc = 0.94$ ) in air ( $Pr = 0.71$ )  $\omega t = 0.2$ ,  $\omega = 10$ , and  $\varepsilon = 0.02$  for different values of  $Gr, Gc$  and  $Df$

$$q_w^* = -k \frac{\partial T^*}{\partial y^*} \bigg|_{y^*=0} \quad (26)$$

Now, where  $y^*$  is the direction of the normal to the surface of the body. Putting equations (12) and (15), the dimensionless coefficient of heat transfer can be calculated as follows:

$$q = \frac{q_w^* \nu}{k V_0^* (T_w^* - T_0^*)} = - \frac{\partial \theta}{\partial y} \bigg|_{y=0} \quad (27)$$

Considering the amplitude and phase, the rate of heat transfer can be written as:

$q = B_5 m_1 - B_4 m_2 + |N| \cos(\omega t + \phi)$ . Where Amplitude is  $|N| = |N_r + i N_i|$  and The phase, the rate of heat transfer is

$$\tan \phi = \frac{N_i}{N_r}$$

$$\text{Where, } N = N_r + i N_i = B_{14} m_1 - B_{15} m_2 + B_{16} m_3 - B_{17} m_4 - B_{18} S c - B_{19} m_6 + B_{20} m_7$$

## 4. Discussion

The effect of thermal diffusion in natural convection flows is very important in many applications. The formulations may be examined to indicate the nature of the interaction of the various contributing terms to buoyancy. For the purpose of this analysis our discussion will be restricted to the aiding or favorable case only. Then, for fluid with Prandtl number  $Pr = 0.71$  which represent air at  $20^\circ\text{C}$  at 1 atmosphere. Chosen the value of the Schmidt number,  $Sc$  to represent the presence of species Carbon dioxide in air ( $Sc = 0.94$ ). Then, the values of  $Gr$  and  $Gc$  are selected arbitrarily. We take  $Gr, Gc > 0$ , that correspond to the cooling of the plate by free convection currents. It is also important to note that negative value of  $A$  leads to suction through the porous boundary plate while positive values depict injection through the heated plate  $y=0$ . The velocity profiles for the binary mixture of air and carbon dioxide are presented in figs 1-4. Now, it is observed from the figures that the velocity increases rapidly near the heated plate, attains a maximum value and then decreases exponentially toward the cold plate. Also, figure 1 show that increasing  $\lambda$  lead to decrease in the velocity, at same time increase  $Gr$  leads to little increase in the velocity and increasing  $Gc$ , also leads to more increase in the same velocity. We may said that increase in  $Gr$  or  $Gc$  leads to corresponding increase in velocity. This is physically true since growing  $Gr$  or  $Gc$  enhances the buoyancy of the fluid and strengthens the convection currents which eventually increase the velocity. The figure further shows that an increase in  $\lambda$  increases the

slip velocity on the porous plate while the velocity of the fluid decreases. The effect of the Dufour parameter on the hydrodynamics is the subject of figure 2. The figure shows that an increase in velocity is achieved by growing the Dufour parameter. The figure further reveals that the effect of velocity slip on the wall could be controlled by varying the buoyancy parameters  $Gr$  and  $Gc$  since increase in  $Gr$  and/or  $Gc$  also acts to support and increase the boundary slip on the surface of the porous plate. The effect of the suction /injection parameter  $A$  on the hydrodynamics is shown in figure 3. The figure shows that the velocity remain constant with the increase of suction parameter  $A$ . From figure 1 and 3, it could be observed that the slip velocity increases near the boundary plate as  $\lambda$  increases. However, due to rare faction of the fluid, the velocity of fluid away from the boundary surface decreases with growing  $Gr$ . It was also observed that fixed values of  $Gc$ ,  $\lambda$  and  $\omega t$ , the velocity of the binary mixture of carbon dioxide in air increases with growing  $Gr$  due to cooling of the plate by free convection currents. In figure 4, it is observed that fluid velocity induced by constant heat and solute inputs on the boundary ( $\omega t = 0$ ) is higher, while it decreases as the oscillation sets in at the thermal as well as concentration boundary condition ( $\omega t = \pi / 2$ ).

Fig.5 shows that the temperature of the fluid decreases with increase in  $\lambda$  and this is caused by the increase in the molecular distance of the fluid particles which acts against thermal diffusion within the fluid. The figure further shows that fluid temperature decreases as the Dufour number increases. The mean skin-friction of carbon dioxide for air is shown in Fig.6. It is observed from this figure that the mean skin-friction decreases with increasing Dufour parameter. Also, the mean skin-friction increase due to the increase in  $Gr$  or  $Gc$  or both. Furthermore, it may be concluded that the mean skin-friction increases with more cooling of the plate by free convection currents.

The amplitude  $|M|$  of the skin-friction for  $\text{CO}_2$  in air is shown in Fig.7. It is evident from this figure that amplitude increases with decreasing  $\lambda$  while an increase in  $Gr$  or  $Gc$  leads to an increase in amplitude of skin-friction on the boundary plate. The effect of  $Df$  on the amplitude of skin-friction shows an increase in the amplitude as  $Df$  increases. However, as  $\lambda$  increases the effect of  $Df$  on the amplitude of the skin-friction becomes negligible.

The temperature profile is presented in Fig.8 for variation in suction parameter and frequency of periodic boundary condition. From this figure it is observed that temperature increases with increase in the  $A$  (injection parameter) while decreases with the increase of frequency of periodic heating  $\omega$ . This figure shows that the values of temperature are greater in vicinity of the heated plate and decreases exponentially toward the cold plate.

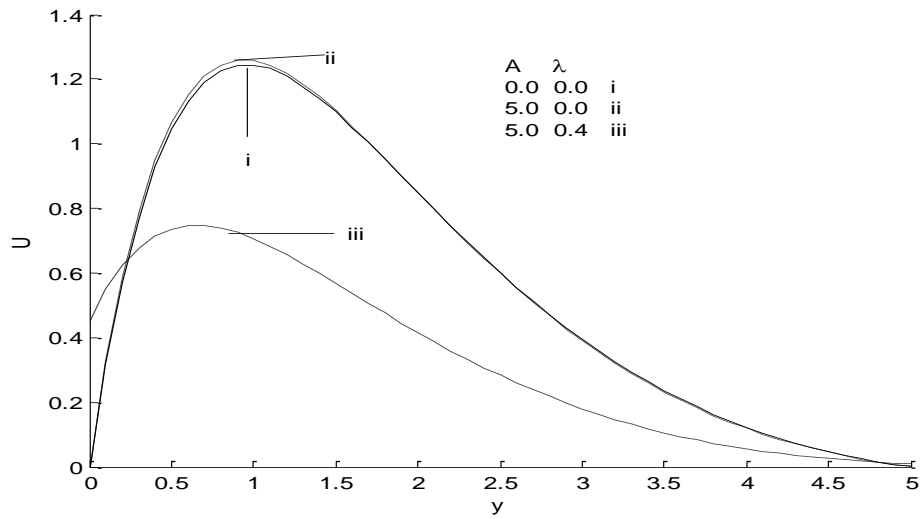


**Figure 3.** Velocity profiles of carbon dioxide ( $Sc=0.94$ ) in air ( $Pr=0.71$ ) for  $Gr=2.0$ ,  $Gc=2.0$ ,  $\omega t=0.2$ ,  $\omega=10$ , and  $\varepsilon=0.02$

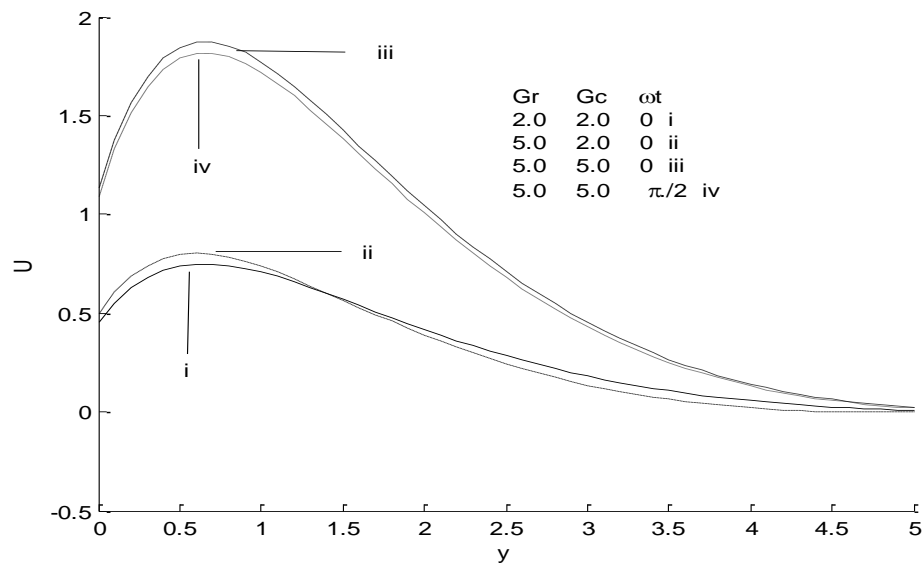


**Figure 4.** Velocity profiles of carbon dioxide ( $Sc=0.94$ ) in air ( $Pr=0.71$ ) for  $A=5$ ,  $\lambda=0.4$ ,  $Gr=10$ , and  $\varepsilon=0.02$

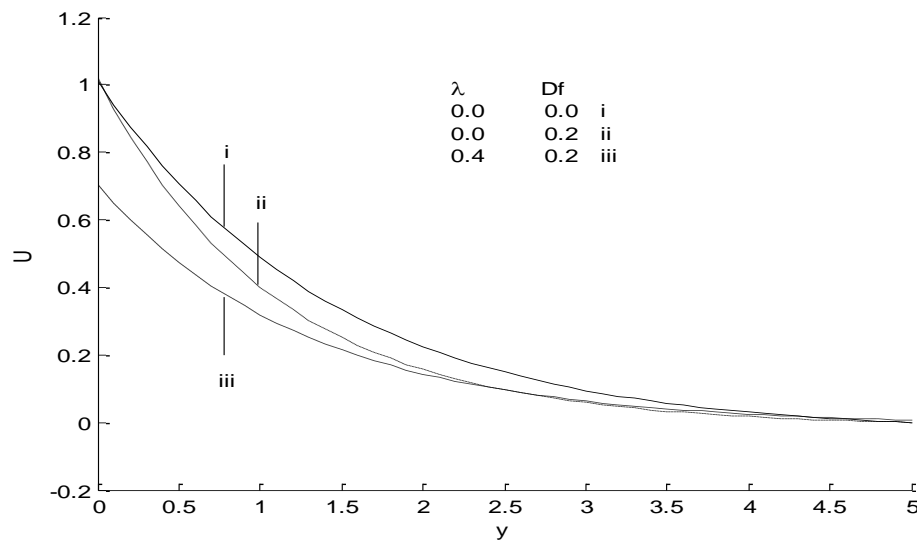


**Figure 5.** Temperature profiles of carbon dioxide ( $Sc=0.94$ ) in air ( $Pr=0.71$ ) for  $A=5$ ,  $\lambda=0.4$ ,  $Gr=10$ , and  $\varepsilon=0.02$

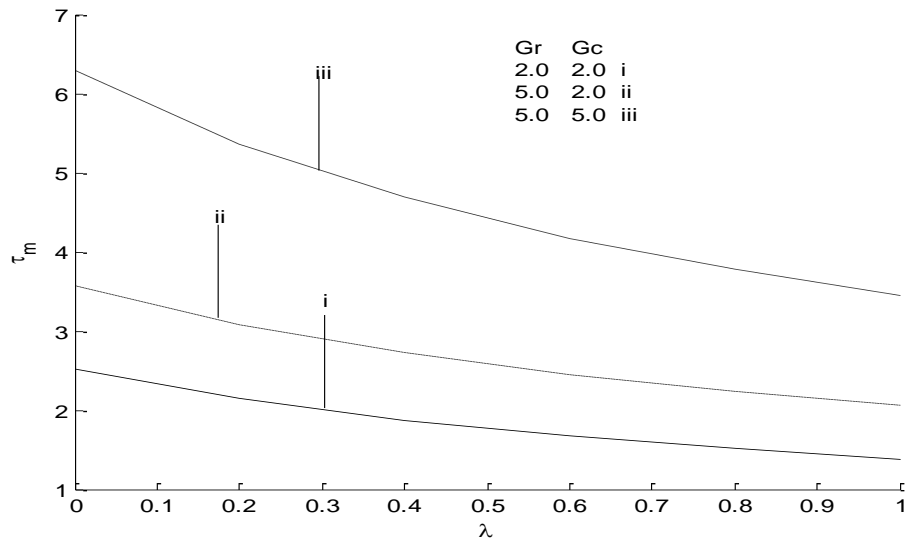


**Figure 6.** The mean skin-friction of carbon dioxide ( $Sc=0.94$ ) for (air)  $Pr=0.71$

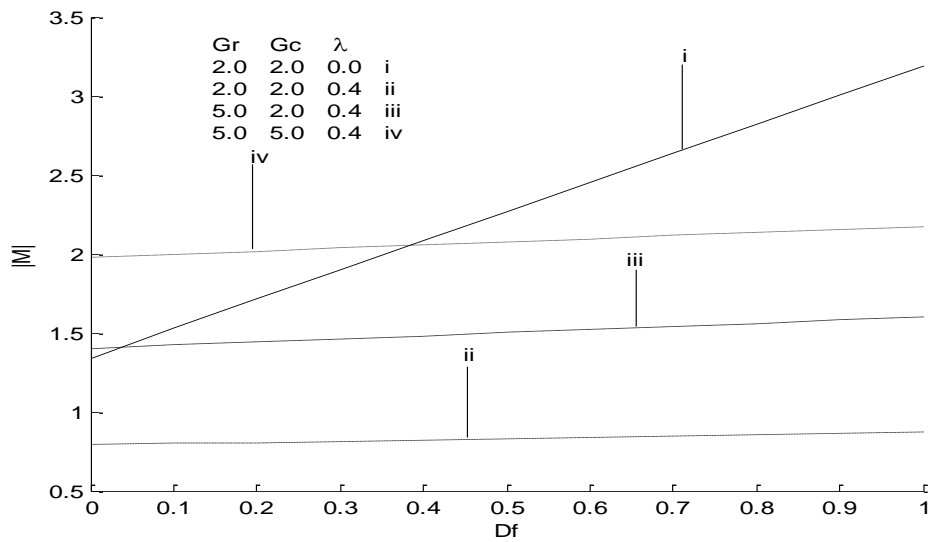


**Figure 7.** The amplitude of skin-friction of carbon dioxide ( $Sc=0.94$ ) in air ( $Pr=0.71$ ) for  $\omega=10$

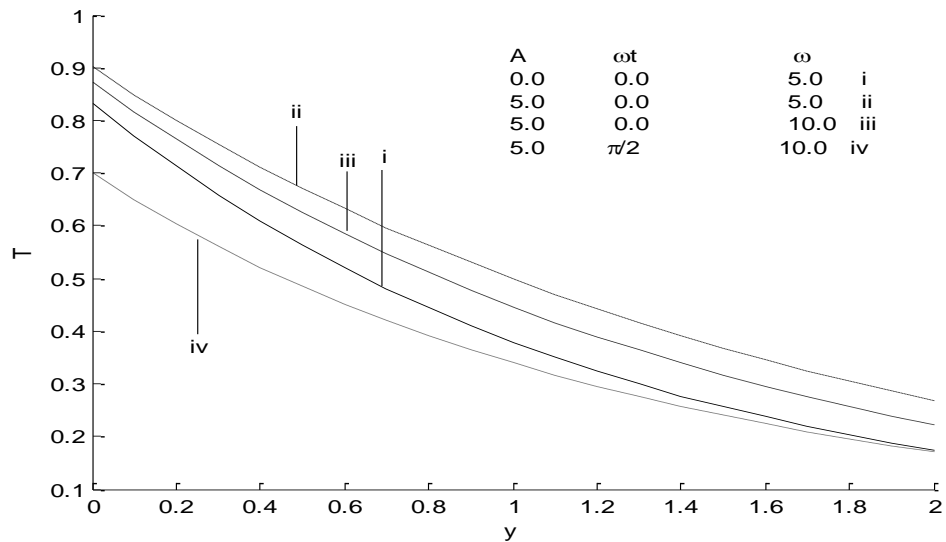


**Figure 8.** The temperature profiles for (air)  $Pr = 0.71$  and  $\epsilon = 0.02$

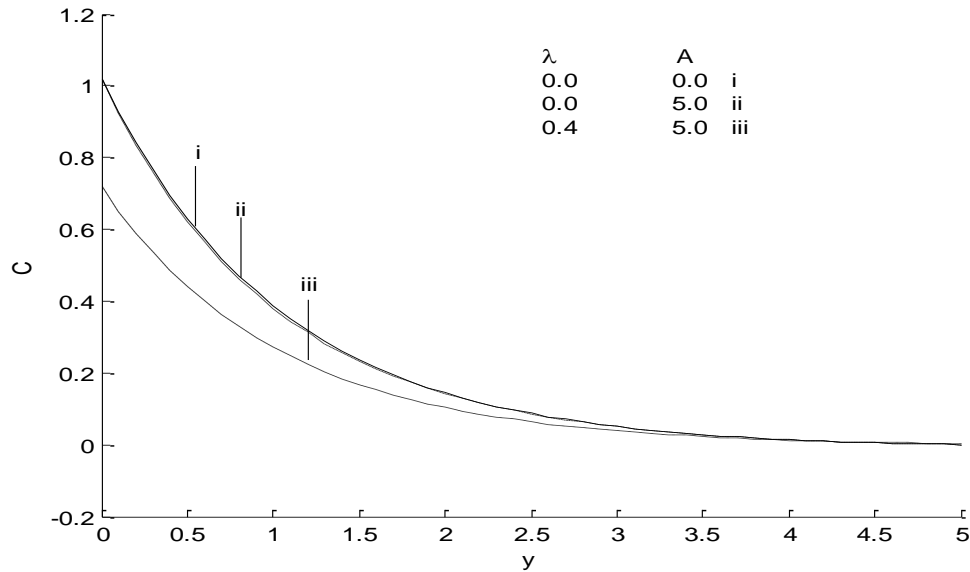


**Figure 9.** The concentration profile of carbon dioxide ( $Sc = 0.94$ ) for  $Gr = 10$  and  $\varepsilon = 0.02$

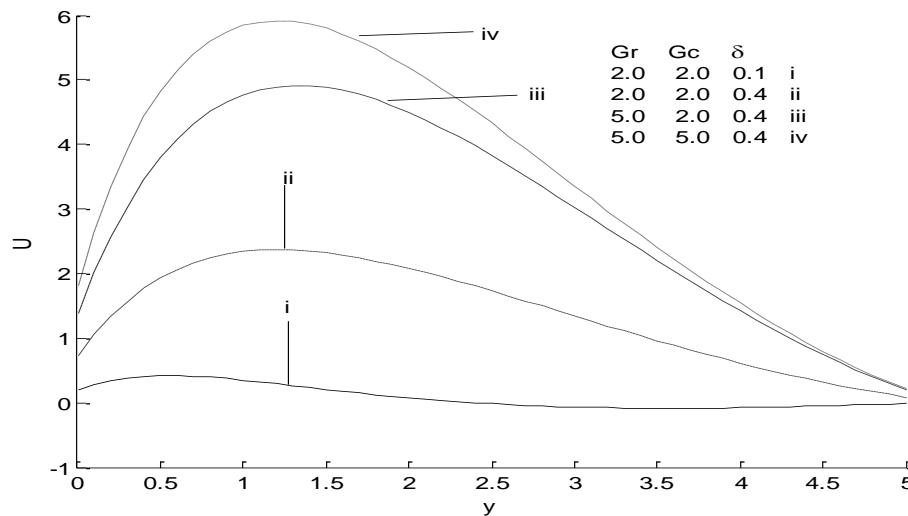


**Figure 10.** The velocity profiles of carbon dioxide ( $Sc = 0.94$ ) in air ( $Pr = 0.71$ ) for  $A = 5$ ,  $\lambda = 0.4$ ,  $Gr = 10$ , and  $\varepsilon = 0.02$

Concentration profile of carbon dioxide is presented in Fig.9 for different  $Kn$  and suction parameter  $A$ . The concentration decreases with increasing  $A$  (suction parameter). It is also evident that the concentration decreases with increasing  $Kn$  (rarefaction parameter). It is discovered that concentration decreases exponentially towards the cold plate.

Now, figure 10 shows that increase in  $Gr$  or  $Gc$  leads to corresponding increase in velocity. Because, it is physically true since growing  $Gr$  or  $Gc$  enhances the buoyancy of the fluid and strengthens the convection currents which eventually increase the velocity. The figure further reveals that an increase in the heat generating parameter  $\delta$  increases the velocity within the channels. This physical fact is attributed to the heat generation which grows the fluid temperature and hence strengthen the convection current which act to increase the fluid velocity.

Now, the numerical values of the phase of skin-friction are presented in table 1. It is observed that the phase of skin-friction increases with increasing  $A$ , this also reveals that increasing  $Df$  and  $\delta$  leads to increase in the phase of the skin-friction while reverse effect is observed for  $\lambda$ , hence, the phase of skin-friction decreases with the increase of  $\lambda$ . The amplitude  $|N|$  and phase ( $\tan\phi$ ) of rate of heat transfer are presented in table 2. This table shows that the amplitude of rate of heat transfer  $|N|$  increases with growing injection parameter while it increases when increasing frequency  $\omega$  on the other hand, the phase of rate of heat transfer ( $\tan\phi$ ) decreases with increase in the injection through the heated plate parameter while it increases as  $(\omega)$  increases.

**Table 1.** The phase of the skin-friction ( $\tan \phi$ ) for carbon dioxide ( $Sc = 0.94$ )  $\omega = 10$  and  $Pr = 0.71$ 

$A$	$Gr = 2, Gc = 2$ $\lambda = 0, \delta = 0.1$ $Df = 0$	$Gr = 2, Gc = 2$ $\lambda = 0.4, \delta = 0.1$ $Df = 0.0$	$Gr = 2, Gc = 2$ $\lambda = 0.4, \delta = 0.1$ $Df = 0.2$	$Gr = 2, Gc = 2$ $\lambda = 0.4, \delta = 0.2$ $Df = 0.2$
0.0	0.7171	0.3395	0.3883	0.4069
0.2	0.8252	0.3944	0.4247	0.4036
0.4	0.9426	0.4504	0.4613	0.4003
0.6	1.0707	0.5075	0.4980	0.3969
0.8	1.2110	0.5658	0.5348	0.3935
1.0	1.3652	0.6253	0.5718	0.3901

**Table 2.** The amplitude and phase of rate of heat transfer

$A$	$\omega = 5$ $ N $	$\omega = 10$ $ N $	$\omega = 5$ $\tan \phi$	$\omega = 10$ $\tan \phi$
0.0	0.9180	1.1796	0.6643	0.8709
0.2	0.9465	1.1965	0.7301	0.9034
0.4	0.9764	1.2137	0.7959	0.9359
0.6	1.0077	1.2311	0.8617	0.9684
0.8	1.0401	1.2488	0.9275	1.0109
1.0	1.0737	1.2666	0.9933	1.0335

## 5. Conclusions

The effect of Dufour on Natural convection double-diffusive flow of heat generating fluid in a vertical channel was examined. Three partial differential equations were used representing velocity temperature and concentration. While, perturbation method was used to solve the equations. During the course of investigation, it is found that as  $\lambda$  increases the velocity slip increases on the boundary plate while the fluid velocity decreases within the channel. Also, the velocity increases with increasing  $Gr, Gc$ ,  $Df$  and  $\delta$ . In addition, the mean skin-friction  $|M|$ , amplitude and the phase of the rate of heat transfer  $|N|$  increases with increases in  $\delta, Df$ , and  $\omega$ , while increases  $\lambda$  and  $\tan \phi$  leads to decreases in it. The temperature and concentration both are increases near the hot plate and decreases exponentially far away from the cold plate.

## Nomenclature and Greek Letters

### Nomenclature

$A$	suction parameter.
$C$	dimensionless species concentration
$C^*$	dimensional species concentration
$C_p$	specific heat at constant pressure,
$C_0^*$	dimensional species concentration at the heated wall

$C_\omega^*$	dimensional concentration at the wall,
$C_\infty^*$	dimensional species concentration of in free stream,
$Df$	Dufour parameter,
$D_m$	molecular diffusivity of the species.
$g$	acceleration due to gravity,
$Gc$	modified Grashof member.
$Gr$	Grashof number.
$h^*$	dimensional gap between the plates,
$H$	dimensionless channel gap
$Kn$	rarefaction parameter,
$K$	thermal conductivity,
$ M $	amplitude of skin friction.
$ N $	amplitude of rate of heat transfer
$Nu$	Nusselt number
$Pr$	Prandtl number
$q$	rate of heat transfer.
$q_\omega^*$	heat flux at the wall,
$Q_0$	Dimensional heat generation coefficient
$Sc$	Schmidt number.
$t$	dimensionless time.
$t^*$	dimensional time,
$T^*$	dimensional temperature.
$T_0^*$	dimensional temperatur at the heated wall
$T_\omega^*$	dimensional temperature of wall.

$T_{\infty}^*$	dimensional temperature of fluid in free stream,	$\beta^*$	coefficient of concentration expansion,
$U$	dimensionless velocity,	$\varepsilon$	amplitude ( $\varepsilon \ll 1$ ),
$U^*$	dimensional velocity,	$\lambda$	Slip/ jump parameter
$V$	suction velocity,	$\theta$	dimensionless temperature,
$V_0$	suction velocity scale	$\nu$	kinematic viscosity
$V^*$	dimensional suction velocity	$\alpha$	thermal diffusivity,
$x^*$	Dimensional distance along the plate	$\tau$	dimensionless shear stress,
$y^*$	Dimensional distance perpendicular to the plate	$\tau^*$	shear stress,
<b>Greek letters</b>		$\rho$	Fluid density,
		$\omega$	frequency
		$\delta$	Heat generation parameter
		$\Delta$	Delta
$\beta$	coefficient of thermal expansion,		

## Appendix

$$m_1 = \frac{-\text{Pr} + \sqrt{\text{Pr}^2 - 4\delta}}{2}, \quad m_2 = \frac{\text{Pr} + \sqrt{\text{Pr}^2 - 4\delta}}{2}, \quad m_3 = \frac{-Sc + \sqrt{Sc^2 + i\omega Sc}}{2}$$

$$m_4 = \frac{Sc + \sqrt{Sc^2 + i\omega Sc}}{2}, \quad m_5 = \frac{-\text{Pr} + \sqrt{\text{Pr}^2 + i\omega \text{Pr} - 4\delta}}{2}, \quad m_6 = \frac{\text{Pr} + \sqrt{\text{Pr}^2 + i\omega \text{Pr} - 4\delta}}{2}$$

$$m_7 = \frac{-1 + \sqrt{1 + i\omega}}{2}, \quad m_8 = \frac{1 + \sqrt{1 + i\omega}}{2}$$

$$B_1 = \frac{1}{(\lambda + 1) - (1 - \lambda)e^{(-ScH)}}, \quad B_2 = -B_1(1 - \lambda)e^{-ScH}, \quad B_3 = \frac{DfB_1Sc^2}{Sc^2 - \text{Pr}Sc + \delta}$$

$$B_4 = \frac{(\text{Pr} + B_3(\lambda + \text{Pr}))(\text{Pr} + \lambda m_1)e^{m_1H} - B_3(\text{Pr} - \lambda Sc)(\text{Pr} - \lambda m_1)e^{-ScH}}{(\text{Pr} + \lambda m_2)(\text{Pr} + \lambda m_1)e^{m_1H} - (\text{Pr} - \lambda m_2)(\text{Pr} - \lambda m_1)e^{-m_2H}},$$

$$B_5 = \frac{\text{Pr} + B_3(\lambda Sc + \text{Pr}) - B_4(\text{Pr} - \lambda m_2)}{(\text{Pr} - \lambda m_1)}, \quad B_6 = \frac{-B_5Gr}{m_1^2 + m_1}, \quad B_7 = \frac{-B_4Gr}{m_2^2 - m_2}, \quad B_8 = \frac{B_3Gr - B_1Gc}{Sc^2 - Sc}$$

$$B_9 = \frac{B_6((\lambda m_1 - 1) + (\lambda m_1 + 1)e^{m_1H}) - B_7((\lambda m_2 + 1) + (\lambda m_2 - 1)e^{-m_2H}) - B_8((\lambda Sc + 1) + (\lambda Sc - 1)e^{-ScH}) - B_2Gc(2\lambda + H)}{(1 + \lambda) - (1 - \lambda)e^{-H}}$$

$$B_{10} = B_6(\lambda m_1 - 1) - B_7(\lambda m_2 + 1) - B_8(\lambda Sc + 1) - B_9(1 + \lambda) - B_2Gc\lambda$$

$$B_{11} = \frac{4iAScB_1}{\omega}, \quad B_{12} = \frac{Sc((1 - B_{11})(\lambda + 1)(Sc + \lambda m_3)e^{m_3H} - B_{11}(\lambda - 1)(Sc - \lambda m_3)e^{-ScH})}{(Sc + \lambda m_4)(Sc + \lambda m_3)e^{m_3H} - (Sc + \lambda m_4)(Sc - \lambda m_3)e^{-ScH}}$$

$$B_{13} = \frac{(1/Sc^2)(Sc - B_{11}Sc(\lambda + 1)) - B_{12}(Sc + \lambda m_4)}{(Sc - \lambda m_3)}, \quad B_{14} = \frac{-B_5m_1A\text{Pr}}{m_1^2 + m_1\text{Pr} - \frac{(\text{Pr}\omega i - 4\delta)}{4}}$$

$$B_{15} = \frac{B_4m_2A\text{Pr}}{m_2^2 - m_2\text{Pr} - \frac{(\text{Pr}\omega i - 4\delta)}{4}}, \quad B_{16} = \frac{-B_{13}m_3^2Df}{m_3^2 + m_3\text{Pr} - \frac{(\text{Pr}\omega i - 4\delta)}{4}}, \quad B_{17} = \frac{-B_{12}m_4^2Df}{m_4^2 - m_4\text{Pr} - \frac{(\text{Pr}\omega i - 4\delta)}{4}}$$

$$B_{18} = \frac{-(B_3A\text{Pr}Sc + B_{11}DfSc^2)}{Sc^2 - Sc\text{Pr} - \frac{(i\omega\text{Pr} - 4\delta)}{4}}$$

$$\begin{aligned}
& \{ B_{14}((Pr + \lambda m_5)(\lambda m_1 - Pr)e^{m_5 H} + (Pr + \lambda m_5)(\lambda m_1 - Pr)e^{m_1 H}) + \\
& B_{15}((Pr + \lambda m_5)(\lambda m_2 - Pr)e^{m_5 H} + (\lambda m_2 - Pr)(-\lambda m_5 + Pr)e^{-m_2 H}) + \\
& B_{16}((Pr + \lambda m_5)(\lambda m_3 - Pr)e^{m_5 H} + (Pr + \lambda m_3)(Pr - \lambda m_5)e^{m_3 H}) - \\
& B_{17}((Pr + \lambda m_5)(\lambda m_4 + Pr)e^{m_5 H} + (Pr + \lambda m_4)(Pr - \lambda m_1)e^{-m_4 H}) - \\
& B_{18}((Pr + \lambda m_5)(\lambda Sc + Pr)e^{m_5 H} + (\lambda Sc - Pr)(Pr - \lambda m_5)e^{-Sc H}) - Pr(Pr + \lambda m_5)e^{m_5 H} \} \\
B_{19} = & \frac{((Pr + \lambda m_5)(\lambda m_6 + Pr)e^{m_5 H} + (Pr - \lambda m_5)(Pr - \lambda m_6)e^{-m_6 H})}{((Pr + \lambda m_5)(\lambda m_6 + Pr)e^{m_5 H} + (Pr - \lambda m_5)(Pr - \lambda m_6)e^{-m_6 H})} \\
B_{20} = & \frac{B_{14}(\lambda m_1 - Pr) - B_{15}(Pr + \lambda m_2) - B_{16}(\lambda m_3 - Pr) - B_{17}(Pr + \lambda m_4) - B_{18}(Pr + \lambda Sc) - B_{19}(Pr + \lambda m_6) + Pr}{(Pr - \lambda m_5)}, \\
B_{21} = & \frac{-(B_6 A m_1 + B_{14} Gr)}{m_1^2 + m_1 - \frac{i\omega}{4}} & B_{22} = \frac{-B_{15} Gr + B_7 m_2 A}{m_2^2 - m_2 - \frac{i\omega}{4}} \\
B_{23} = & \frac{-(B_{13} Gc + B_{16} Gr)}{m_3^2 + m_3 - \frac{i\omega}{4}} & B_{24} = \frac{-(B_{17} Gr + B_{12} Gc)}{m_4^2 - m_4 - \frac{i\omega}{4}} \\
B_{25} = & \frac{-B_{20} Gr}{m_5^2 + m_5 - \frac{i\omega}{4}} & B_{26} = \frac{-B_{19} Gr}{m_6^2 - m_6 - \frac{i\omega}{4}} \\
B_{27} = & \frac{-(Gc B_{11} - B_8 A Sc + B_{18} Gr)}{Sc^2 - Sc - \frac{i\omega}{4}} & B_{28} = \frac{4i B_9 A}{\omega} & B_{29} = \frac{4B_2 Gc A}{4 - i\omega y} \\
& \{ B_{21}((1 + \lambda m_7)(\lambda m_1 - 1)e^{m_7 H} + (1 - \lambda m_7)(\lambda m_1 + 1)e^{m_1 H}) - \\
& B_{22}((1 + \lambda m_7)(\lambda m_2 + 1)e^{m_7 H} + (\lambda m_2 - 1)(1 - \lambda m_7)e^{-m_2 H}) + \\
& B_{23}((1 + \lambda m_7)(\lambda m_3 - 1)e^{m_7 H} + (1 + \lambda m_3)(1 - \lambda m_7)e^{m_3 H}) - \\
& B_{24}((1 + \lambda m_7)(\lambda m_4 + 1)e^{m_7 H} + (\lambda m_4 - 1)(1 - \lambda m_7)e^{-m_4 H}) + \\
& B_{25}((1 + \lambda m_7)(\lambda m_5 - 1)e^{m_7 H} + (\lambda m_5 + 1)(1 - \lambda m_7)e^{m_5 H}) - \\
& B_{26}((1 + \lambda m_7)(\lambda m_6 + 1)e^{m_7 H} + (\lambda m_6 - 1)(1 - \lambda m_7)e^{-m_6 H}) - \\
& B_{27}((1 + \lambda Sc)(\lambda m_7 + 1)e^{m_7 H} + (\lambda Sc - 1)(1 - \lambda m_7)e^{-Sc H}) - \\
& B_{28}((1 + \lambda)(\lambda m_7 + 1)e^{m_7 H} + (\lambda - 1)(1 - \lambda m_7)e^{-H}) + \\
& B_{29}((\lambda)(\lambda m_7 + 1)e^{m_7 H} + (1 + \lambda)(1 - \lambda m_7)e^{-m_6 H}) \} \\
B_{30} = & \frac{((1 + \lambda m_8)(\lambda m_7 + 1)e^{m_7 H} - (1 - \lambda m_8)(1 - \lambda m_7)e^{-m_8 H})}{((1 + \lambda m_8)(\lambda m_7 + 1)e^{m_7 H} - (1 - \lambda m_8)(1 - \lambda m_7)e^{-m_8 H})} \\
& B_{21}(\lambda m_1 - 1) - B_{22}(1 + \lambda m_2) - B_{23}(\lambda m_3 - 1) - B_{24}(1 + \lambda m_4) + B_{25}(\lambda m_5 - 1) - \\
& B_{26}(1 + \lambda m_6) - B_{27}(\lambda Sc + 1) - B_{28}(\lambda + 1) + B_{29}(\lambda) - B_{30}(1 + \lambda m_8) \\
B_{31} = & \frac{B_{26}(1 + \lambda m_6) - B_{27}(\lambda Sc + 1) - B_{28}(\lambda + 1) + B_{29}(\lambda) - B_{30}(1 + \lambda m_8)}{(1 - \lambda m_7)},
\end{aligned}$$

## REFERENCES

- 
- [1] Marcos J. D., Izquierdo M., and Parra D., *Solar space heating and cooling for Spanish housing potential energy earnings and emissions reduction*. Sol. Energy, 85(2011), 2622-2641.
- [2] Ghadelar N., Ghali K., and Chehaitly S., *assessing thermal comfort of active people in transitional spaces in presence of air movement*. Energy Build 43(2011), 2832-2842.
- [3] Vijayavenkatarama S., Iniyan S., and Goic R., *A review of solar drying technologies* Renew Suet. Energy Rev. 16(2012), 2832-2842.
- [4] Serrano-Arellano J., Xaman J. and Aluarez G., *Optimum*

- ventilation based on the ventilation effectiveness temperature and CO<sub>2</sub> distribution ventilated cavities. *Int. J. Heat mass Transfer*, 62(2013), 9-21.
- [5] Xu H. T., Wang Z. Y., Kerimi F., Yanga M., and Zhang. *Numerical Simulation of diffusive mixed convection in an open enclosure with different cylinder locations*. *Int. Commun. Heat Mass Transfer* 52(2014), 35-45.
- [6] Boutana N., Bohloul A., Vasseur P., and Joly F., *Soret and double-diffusive convection in a porous cavity*. *J. Porous Med.* 52(2004), 41-57.
- [7] Nithyaderi N. and Yang R. J., *Double-diffusive natural convection in a partially heated enclosure with Soret and Dufour effects*. *Int. J. Heat Fluid flows*, 30(2009), 902-910.
- [8] Jha B. K., Joseph S. B., and Ajibade A. O., Role of thermal diffusive on double-diffusive natural convection in a vertical annular porous Medium. *Ain Shams Engineering Journal*. 6(2), (2015), 629-637.
- [9] Jha B. K., and Ajibade A. O., Free convective flow of heat generating absorbing fluid between vertical porous plate with periodic heat input. *Int. Commun. Heat mass Transfer* 19(36), (2009), 624-631.
- [10] Hayat T., Hussan M., Awais M., and Obaidat S., *Melting heat transfer in a boundary layer flow of a second grade fluid under Soret and Dufour effect*, *International Journal of Numerical Method for Heat and fluid flow* 23(7), (2013), 1155-1160.
- [11] Jha, B.K and Ajibade, A.O., *Free convection flow between Heat And Mass Transfer Flow in a vertical Channel with Dufour effect*, *Journal of process Mechanical Engineering*, 224(2), (2010), 91-101.
- [12] Ajibade, A.O., *Dual-phase-lag and dufour effects on unsteady double-diffusive convection flow in a vertical micro-channel filled with porous material*, *J. process Mech. Eng.*, 228(4), (2013). 272-285.
- [13] Sharma P. K., *Influence of periodic temperature and concentration on unsteady free convection viscous incompressible flow and heat transfer past a vertical plate in slip-flow regime*. *Matematicas*. 13(1). (2005), 51-62.
- [14] Srinivasa, A. H. and Eswara, A. T., *Unsteady free convection flow and heat transfer from an isothermal truncated cone with variable viscosity*, *Int. J. Heat Mass Transfer*, 57, (2013), 411-420.
- [15] Hossian, M.A., Hussaini, S. and Rees, D.A.S., *Influence of fluctuating surface temperature and concentration on natural convection flow from a vertical flat plate*, *ZAMM*. 81, (2001), 699 – 709.
- [16] Sharma, P.K. and Chaudhary, R.C., *Effect of variable suction on transient free convection viscous incompressible flow past a vertical plate with periodic temperature variation in slip flow regime*, *Emirate Journal for Engineering Research*, 8(2), (2003), 33 – 38.
- [17] Anwar, K., *MHD unsteady free convective flow past a vertical porous plate*, *ZAMM*, 78, (1998), 73-80.
- [18] Soundalgekar, V. M., Wavre. P.D. *Unsteady free convection flow past an infinite vertical plate with constant suction and mass transfer* *Int. J. Heat Mass Transfer*, 20, (1977), 1363 – 1373.
- [19] Soundalgekar, V. M., Wavre. P.D., *Unsteady free convection flow past an infinite vertical plate with suction and mass transfer*, *Int. J. Heat Mass Transfer*, 20. (1977), 1375 – 1380.
- [20] Chen, T.S. Yuh, C.F., Montsoglon, A. *The combined heat and mass transfer in mixed convective along an inclined plate*, *Int. J. Heat Mass Transfer*. 23, (1980)527 – 537.
- [21] Haddad O. M., Abuzaid M. M., and Al-Nimir M. A., *Developing free convective gas flow in a vertical open-ended Micro-Channel fill with a porous media*. *Numeral Heat transfer part A: Appl* 48, (2005), 693-710.
- [22] Haddad O. M., Al-Nimir M. A., and Al-Omary J. Sh., *Free convection of gaseous slip flow in porous Micro-Channel Under local thermal Non-equilibrium condition*. *Trans. Porous media* 67, (2007), 453-471.
- [23] Ogulata R. T. and Dabo F., *Experiment and entropy generation minimization analysis of a cross flow heat exchanger*. *Int. J. Heat Mass Transfer* 41, (1997), 373-381.
- [24] Caliskan S., *Flow and heat transfer characteristics of transverse perforated rids under impingement jets*, *Int. J. Heat Mass Transfer* 66, (2013), 244-260.
- [25] Abdelaal M. R. and Jog M. A., *Heat/mass transport in a drop translating in time-periodic electric field*. *Int. J. Heat Mass Transfer* 66, (2013), 284-294.
- [26] Zambra C. E. and Moraga N. O., *Heat and mass transfer in landfills simulation of the pile self-heating and of soil contamination*. *Int. J. Heat Mass Transfer* 66, (2013), 284-294.
- [27] Matti L. and Reijo K., *Conjugate heat transfer in a plate –one surface at constant temperature and the other cooled by forced or natural convection*. *Int. J. Heat Mass Transfer* 66, (2013), 489-495.
- [28] Hadi V. M. and Jerzy M. F., *Maximization of heat transfer across micro-channels*. *Int. J. Heat Mass Transfer* 66, (2013), 517-530.
- [29] Mohamed M. M. and Tassos G. K., *Heat transfer correlation for flow boiling in small to micro tube*. *Int. J. Heat Mass Transfer* 66,(2013), 553-574.
- [30] Alessandra A. and Augusta P., *Mass/heat transfer through laminar boundary layer in ax symmetric micro channels with non uniform cross section and fixed wall concentration/temperature*. *Int. J. Heat Mass Transfer* 68, (2014), 21-28.
- [31] Heui-seol R., *Heat transfer mechanism in pool boiling*. *Int. J. Heat Mass Transfer* 68,(2014), 332-342.
- [32] Heui-seol R., *Heat transfer mechanism in solidification*. *Int. J. Heat Mass Transfer* 68, (2014), 391-400.